Time-Resolved In Situ Spectroscopy During Formation of the GaP/Si(100) Heterointerface

Oliver Supplie,[*,†,‡,¶] Matthias M. May,[‡,¶] Gabi Steinbach,[§] Oleksandr Romanyuk,[‖] Frank Grosse,[⊥] Andreas Nägelein,[†] Peter Kleinschmidt,[†,‡] Sebastian Brückner,[†,‡] and Thomas Hannappel[†,‡]

†*Technische Universität Ilmenau, Institut für Physik, Ilmenau, Germany*

‡*Helmholtz-Zentrum Berlin, Institute for Solar Fuels, Berlin, Germany*

¶*Humboldt-Universität zu Berlin, Institut für Physik, Berlin, Germany*

§*Helmholtz-Zentrum Dresden-Rossendorf, Dresden, Germany*

‖*Institute of Physics, Academy of Sciences of the Czech Republic, Prague, Czech Republic*

⊥*Paul-Drude Institut für Festkörperelektronik, Berlin, Germany*

E-mail: oliver.supplie@tu-ilmenau.de

Abstract

Though III-V/Si(100) heterointerfaces are essential for future epitaxial high-performance devices, their atomic structure is an open historical question. Benchmarking of transient optical in situ spectroscopy during chemical vapor deposition to chemical analysis by X-ray photoelectron spectroscopy enables us to distinguish between formation of surfaces and of the heterointerface. A terrace-related optical anisotropy signal evolves during pulsed GaP nucleation on single-domain Si(100) surfaces. This dielectric anisotropy agrees well with the one calculated for buried GaP/Si(100) interfaces from differently thick GaP epilayers. X-ray photoelectron spectroscopy reveals a chemically shifted contribution of the P and Si emission lines, which quantitatively correspond to one monolayer and establish simultaneously with the nucleation-related optical in situ signal. We attribute that contribution to the existence of Si–P bonds at the buried heterointerface. During further pulsing and annealing in phosphorous ambient, dielectric anisotropies known from atomically well-ordered GaP(100) surfaces superimpose the nucleation-related optical in situ spectra.

Graphical TOC Entry

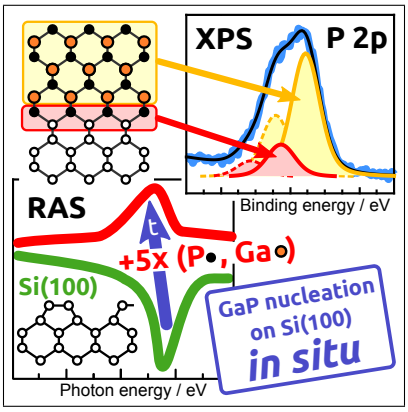

Keywords

Heterointerfaces, III-V on Silicon, optical in situ spectroscopy, photoelectron spectroscopy, MOCVD

Since Kroemer's work in the 1980's,[1,2] it is known that the heterointerface is decisive for future high-performance III-V/Si(100) devices. However, it is still not understood how the interface is formed at the atomic scale. Surface chemistry on the Si surface during III-V nucleation under non-equilibrium conditions will determine the electronic structure across the interface and is essential for defect induction into subsequent epilayers. GaP/Si(100) is the ideal system to study the interface formation, since defects such as antiphase disorder and twinning can experimentally be minimized in GaP/Si(100) heteroepitaxy by an adequate choice of single-domain silicon substrate preparation,[3,4] pulsed GaP nucleation[5–7] and GaP growth parameters.[8] By analyzing the GaP sublattice orientation and the dimer orientation at Si(100) prior to nucleation, an abrupt interface model with a preference for Si–Ga bonds was suggested,[9] but any direct experimental evidence for these bonds was not given. *Ab initio* density functional theory calculations showed that abrupt Si–P are energetically favored over abrupt Si–Ga bonds for a wide range of chemical potentials.[10,11] While compensated interfaces (where the electron counting rule is fulfilled by atomic exchange across the interface) exhibit even lower formation energies,[10] we indirectly found indications for a kinetically limited abrupt interface formation with Si–P bonds from *in situ* reflection anisotropy spectroscopy (RAS).[10] RAS is particularly sensitive to (100) surfaces of cubic crystals[12–14] (see experimental section) and detailed knowledge about RAS signatures and their origins contributes to a microscopic understanding of non-equilibrium interaction mechanisms during metalorganic chemical vapor deposition (MOCVD). Such a dielectric anisotropy was attributed to the GaP/Si(100) heterointerface,[15] but it remained unclear whether it originated in interfacial bonds inducing anisotropic transitions,[16] in in plane anisotropic interfacial strain[17] either at steps or terraces, or in broken symmetry by truncation of the lattice.[18]

In this letter, we analyze changes in the dielectric structure during GaP nucleation on Si(100) time-resolved with optical *in situ* spectroscopy in MOCVD ambient and with *in system* photoelectron spectroscopy for chemical analysis to provide direct evidence for the

binding situation and atomic structure of the GaP/Si(100) heterointerface.

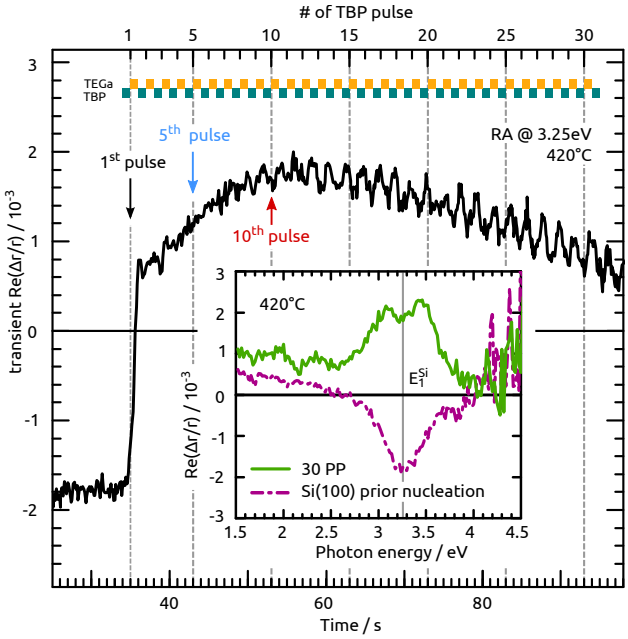

Figure 1: Transient RA measurement at 3.25 eV during 30 pulse pairs consisting of alternating TBP and TEGa pulses (1 s each) on A-type Si(100). The time scale refers to the starting of the measurement after recording the Si(100) RA spectrum shown in the inset (red dash-dotted line), with the first TBP pulse starting at about 34 s. The inset also shows the RA spectrum after 30 (TBP, TEGa) PP (green line).

We started all experiments with an almost single-domain, A-type Si(100) surface (nomenclature according to Chadi[19]) with majority domains consisting of monohydride-terminated dimers oriented perpendicular to the step edges.[3] Such a surface exhibits a terrace-related dielectric anisotropy with a characteristic RAS signal (see inset of Fig. 1, broken violet line), where the sign corresponds to the dimer orientation.[4,20,21] During nucleation, we offer pulse pairs (PP) consisting of alternating tertbutylphosphine (TBP) and triethylgallium (TEGa) pulses for 1 s each. Transient RA at 3.25 eV (slightly below the E_1 interband transition of Si) shows that the anisotropy related to the monohydride-terminated Si(100) surface vanishes with the first TBP pulse and an anisotropy of opposite sign establishes during further pulsing (Fig. 1). Within about the first ten PP, this anisotropy of different sign is increasing while subsequent pulsing leads to a decreasing RAS signal with a modulated oscillation of slightly increasing amplitude. RAS signals also depend on a variety of influences, such as tempera-

ture, strain, internal electric fields, and spectral shifts must be considered when interpreting RA transients. The extinction of the Si(100) dielectric anisotropy during the very first pulse probably is caused by TBP (or fragments of it) being adsorbed on the surface. The arising dielectric anisotropy of opposite sign indicates an ordered surface or well-defined interface formation. A decreasing RA amplitude, in contrast, could correspond to an increased degree of disorder or a spectral shift, while modulated oscillations were interpreted as a periodically created and consumed surface reaction layer.[22] XPS quantification (see below) indicates that one pulse increases the GaP epilayer thickness by about one monolayer (after initial heterointerface formation). The modulation follows indeed the pulsing sequence. The oscillation period seems slightly enlarged, spectral resolution, however, would be necessary to strengthen this observation.

The inset in Fig. 1 also shows the resulting RA spectrum after 30 PP (green line) with two peak-like contributions at about 3.1 eV and 3.5 eV. A partly similar feature was observed during chemical beam epitaxy of GaP on Si(113),[22,23] but its origin remained unclear. In order to resolve the temporal evolution over the whole spectral range, we stopped pulsing after 5 and 10 PP, respectively, to measure RAS at 50 °C and benchmark the spectra to low-energy electron diffraction (LEED) and X-ray photoelectron spectroscopy (XPS).

After 5 PP, the RA spectrum exhibits one clear peak centered at 3.3 eV (Fig. 2(a), blue line) and already a shoulder at the E_1 interband transition of GaP. This RAS signal will be called "nucleation RAS signal" $\frac{\Delta r}{r}\big|_{\text{nucleation}}$ in the following. Compared to monohydride-terminated Si(100) (broken blue line), $\frac{\Delta r}{r}\big|_{\text{nucleation}}$ is shifted about 100 meV towards lower energies and flipped in sign. After 10 PP (broken red line), the dielectric anisotropy increases slightly and is superimposed by an increased contribution at the E_1 interband transition of GaP (spectra were scaled to compensate slight differences in intensity caused by the domain ratio[28]). In order to compare to the nucleation layer directly before actual GaP layer growth, we heated both identical samples subsequently to 595 °C under TBP supply before cooling and desorption of excess P,[29] see Fig. 2(b). The contribution at E_1 of GaP increases, in

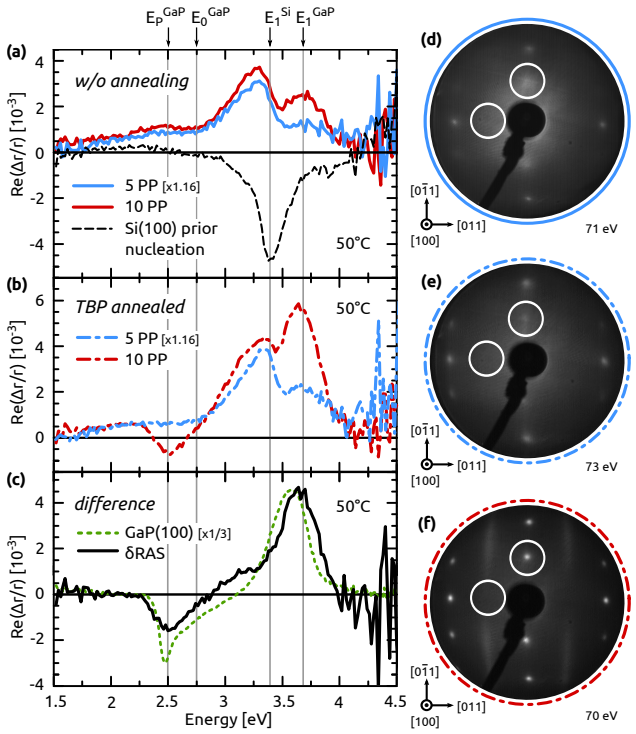

Figure 2: *(a-c) RA spectra measured at 50°C:* (a) After 5 (blue) resp. 10 (red) PP, scaled so that the Si(100) spectra (black dashed line) prior to pulsing match. (b) Identical samples as in (a) which where subsequently heated to 595 °C with TBP supply. (c) Difference RA spectrum (blue line in (a) substracted from red line in (b)) in comparison to a $(2\times2)/c(4\times2)$ reconstructed GaP(100) reference (green dashed line). Grey vertical lines indicate critical point energies of GaP[24] and Si[25] as well as a transition E_P^{GaP} between a surface state of $(2\times2)/c(4\times2)$ reconstructed GaP(100) and the X-valley CBM.[26,27] *(d-f) LEED patterns corresponding to the RA spectra:* (d) after 5 PP, (e) after 5 PP plus annealing in TBP, (f) after 10 PP plus annealing in TBP.

particular for the 10 PP sample, while that at 3.3 eV basically remains unchanged. The LEED pattern of the 5 PP sample in Fig. 2(e) are less diffuse compared to prior annealing and show a weak spot at half order along [0$\bar{1}$1]. In the RA spectrum after 10 PP, $\frac{\Delta r}{r}\big|_{10\,\mathrm{PP}}$, an additional anisotropic contribution occurs at the electronic transition E_P^{GaP} between a surface state (related to the $(2\times2)/c(4\times2)$ reconstruction of GaP(100)) and the GaP conduction band mimimum.[26,27]) Here, we monitor the formation of well ordered GaP/Si(100) surfaces just by pulsing and annealing in TBP. This surface also exhibits a LEED pattern with streaks and spots at half order along [0$\bar{1}$1] in Fig. 2(f) just as for a corresponding GaP(100) surface.[30] Consequently, $\frac{\Delta r}{r}\big|_{10\,\mathrm{PP}}$ is a superposition of a GaP surface signal and $\frac{\Delta r}{r}\big|_{\mathrm{nucleation}}$.

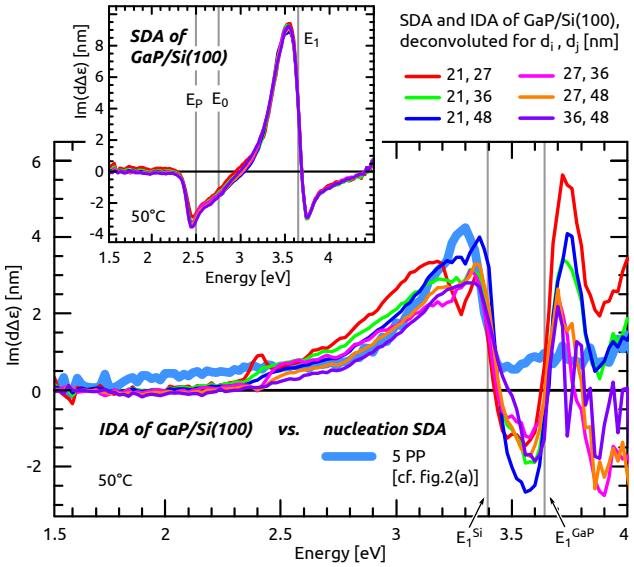

Figure 3: Calculated interface anisotropies from pairs of differently thick, $(2 \times 2)/c(4 \times 2)$ reconstruced GaP epilayers on Si(100) in comparison to the surface dielectric anisotropy of Si(100) with 5 pulse pairs (cf. Fig 2(a), blue line). (inset) Corresponding surface dielectric anisotropies.

This becomes more evident, when comparing the difference spectrum

$$\delta\mathrm{RAS} = \left.\frac{\Delta r}{r}\right|_{10\,\mathrm{PP}} - \left.\frac{\Delta r}{r}\right|_{\mathrm{nucleation}} \tag{1}$$

with that of a $(2 \times 2)/c(4 \times 2)$ reconstructed GaP(100) reference in Fig. 2(c).

The dielectric anisotropy stemming from the surface-modified bulk $\mathrm{E}_1^{\mathrm{GaP}}$ transition develops faster than the surface-state related anisotropy at $\mathrm{E}_P^{\mathrm{GaP}}$ (see Fig. 2). While the GaP/Si(100) surface is not yet well-ordered after 5 pulses, the anisotropy at 3.3 eV is already established [cf. Fig. 2(b)]. This indicates that the interface forms already during the very first pulses at low temperature and not during annealing at higher temperatures, which supports the possibility of a kinetically limited formation of abrupt interfaces.[10]

If $\left.\frac{\Delta r}{r}\right|_{\mathrm{nucleation}}$ originates indeed from the GaP/Si(100) interface rather than from an ordered surface, it should persist during subsequent GaP epilayer growth and contribute to the RA spectra due to internal reflection at the buried interface.[31] The interface dielectric anisotropy (IDA), however, is convoluted with interference and absorption in the RA spec-

tra[15,31] and needs to be separated from the surface dielectric anisotropies (SDA). Within a dielectric model, SDA and buried IDA can be extracted from the RAS data of two differently thick GaP/Si(100) samples i and j (see experimental section for more details).[15] Fig. 3 shows the resulting SDA (inset) and IDA, respectively, for different pairs of GaP epilayer thicknesses (d_i, d_j) grown on A-type Si(100) with 5 PP nucleation. As expected, the lineshape of the SDA for all pairs of samples matches that of $(2\times2)/c(4\times2)$ reconstructed GaP(100) (cf. Ref.[15]). In the following, we will compare the extracted IDA of GaP/Si(100) to the SDA calculated from $\frac{\Delta r}{r}\big|_{\text{nucleation}}$ (cf. Fig. 2(a), solid blue line). The derivative-like feature in the IDA around the E_1 transition of GaP could originate in an interface modification of the GaP bulk transition caused by strain or by the truncation of the GaP lattice at the interface.[18] Note that the SDA (solid blue line) already contains a small superimposed contribution at E_1^{GaP}, which probably is GaP(100) surface- and thus not interface-related (see discussion of Fig. 2). However, at higher photon energies, interpretation of the IDA becomes more difficult due to higher absorption beyond E_1^{GaP} and possible artifacts in the calculation of the IDA.[15] In the following, we will focus on the spectral region around the E_1 transition of Si. Nucleation-related SDA and IDA at that peak match well with only slight variations of the actual lineshape. This suggests that the nucleation anisotropy is indeed arising at the actual GaP/Si(100) heterointerface.

The IDA cannot be caused by Si dimers rotated from A-type towards B-type at Si(100), since this dimer-related anisotropy would not persist during GaP growth but vanish, when the dimers break during nucleation. Nucleation on Si(100) B-type[10] leads to a flip in sign of $\frac{\Delta r}{r}\big|_{\text{nucleation}}$ at 3.3 eV (not shown here), which implies that the dielectric anisotropy is terrace-related. Due to the tetrahedral lattice coordination, Si–P or Si–Ga bonds only exist along [011] direction at abrupt interfaces with (formerly) A-type Si single-domain terraces and even-numbered atomic step height. This anisotropy could cause the IDA, similar to what was suggested for AlAs/GaAs.[16] The existence of an anisotropic density of states at abrupt GaP/Si(100) interfaces was indeed evidenced by DFT.[11] Calculations of the interface-related

interband transitions and the corresponding RA spectra, however, are not available. The energetic position of the maximum peak of $\frac{\Delta r}{r}\big|_{\text{nucleation}}$ is close to the Si E_1 interband transition. Hence, a transition involving interface perturbed Si bulk states seems also feasible as the origin of the signal, in analogy to what is known for surfaces.[18,32] Strain was, for example, suggested to cause the RAS signal of UHV-prepared Si(100).[33] DFT calculations,[10,11] however, revealed interplane relaxations along the [100] direction close to the interface, whereas in-plane relaxations were small for the abrupt interfaces. Further modelling and calculation of RA spectra are necessary to understand the origin of the IDA. Also the influence of varying the chemical ambient during nucleation by different sequences seems highly instructive.

In order to resolve the chemical composition of the heterointerface, we performed XPS measurements of 5 and 10 PP samples after contamination-free sample transfer[34] to UHV. Si–P and Si–Ga interfacial bonds are expected to give additional, chemically shifted contributions in the photoemission (PE) lines of the two species involved in the bond at the interface. Indeed, XPS reveals distinct components for both the Si 2p and P 2p core levels (see fits in Fig. 4). For the P 2p line [Fig. 4(a)], we observe a second spin-orbit split component P_2 after 5 and 10 PP. The P_2 components are chemically shifted towards higher binding energies (E_B) and vanish for thicker epilayers of GaP (cf. gray spectrum in Fig. 4(a)). Hence, P_2 is interface-related. Employing a quantitative model with calculated cross-sections and electron attenuation lengths,[35–37] we find that the P_2 component corresponds to about 1 monolayer (ML) for 5 and 10 PP (see also Fig. 5). The first P contribution, P_1, matches energetically the line position of the thicker sampe (70 s GaP growth) (129.54 eV for the P $2p_{3/2}$, see dotted line in Fig. 4(a)) and is therefore assigned to P in GaP.

For the Si 2p level [Fig. 4(c)], we also observe two peak components after 5 and 10 PP. The larger component, Si_1, corresponds to bulk Si. The smaller component, Si_2, is shifted towards higher E_B. Similarly, the Si 2p core-level was shifted towards higher E_B for Si bound to As in GaAs-on-Si heteroepitaxy.[38] Both oxide species[39] and carbon related species,[40] which might lead to similar shifts, are ruled out by XPS measurements. Si–Ga bonds, in contrast, are

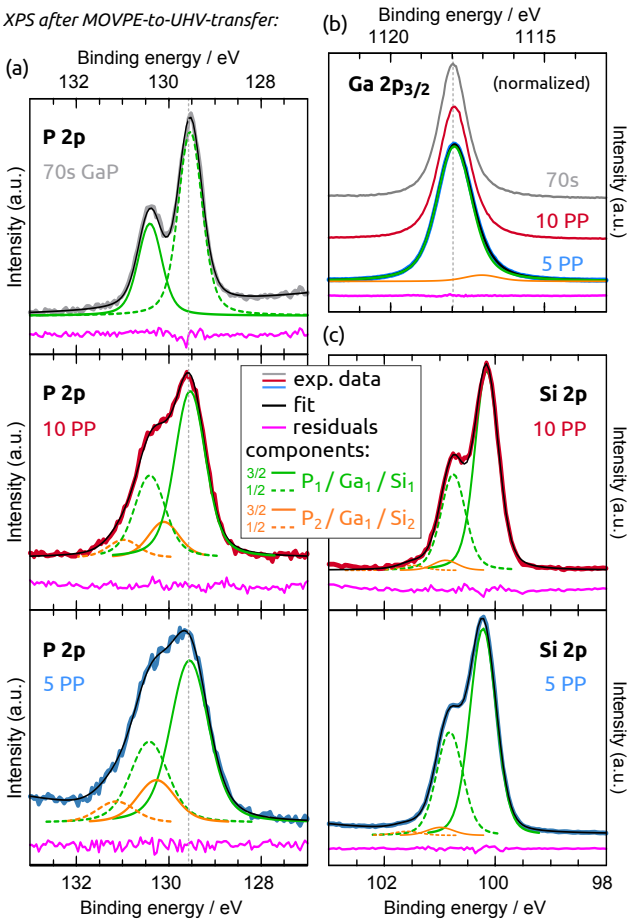

Figure 4: XPS (monochromated Al K_α) at different stages of nucleation (after TBP annealing; blue for 5 PP, red for 10 PP and grey for 70 s GaP growth). (a) P 2p core level region, the vertical dotted line indicates E_B = 129.54 eV. (b) Ga $2p_{3/2}$ PE line (the fit is only shown for 5 PP). The vertical dashed line indicates E_B = 1117.97 eV. (c) Si 2p core level region. Fitted components to the PE lines are shown in green (P_1, Ga_1 resp. Si_1) and orange (P_2, Ga_2 resp. Si_2). Solid and dashed lines represent $2p_{3/2}$ and $2p_{1/2}$ components, respectively. The fit envelope (black line) shown in (a) also includes fitted components for the Si 2p plasmon around 135 eV and the Ga 3p PE line was included for the fit in (c). Residuals are plotted with an offset in pink.

expected to induce a chemical shift towards lower E_B.[38] Quantitatively, we estimate again a coverage of about 1 ML for Si_2, similar to P_2 (see also Fig. 5). This coverage corresponds to one interfacial layer. Consequently, we attribute both Si_2 and P_2 to the GaP/Si interface. The Ga $2p_{3/2}$ PE line of the 5 PP sample in Fig. 4(b) contains a small second component (orange line, about 4 % of the main peak), which is shifted 0.87 eV to lower E_B. We could not detect this component in the other Ga $2p_{3/2}$ and Ga 3p PE lines (not shown here). Possible

origins for this second component are, for example, Ga–Ga bonds at antiphase boundaries (since the preferential A-type Si(100) surface contains small residual B-type domains at the step edges[3] and antiphase boundaries which will not annihilate within the very first MLs) or minority Si–Ga bonds at the heterointerface. These could result from residual Ga on the surface prior to nucleation[10] or a non-ideally abrupt heterointerface. A corresponding Si–Ga component in the Si 2p peak cannot be detected, however, due to the low intensity. A direct evaluation of the Ga 3p and P 2p peak contributions with atomic sensitivity factors reveals that the minor P 2p peak P_2 after 5 and 10 PP quantitatively matches the minor Si_2 signal, while the Ga 3p line is at least a factor of 3 stronger, with an intensity ratio to P_1 of $1(\pm 0.15)$. Hence, we cannot exclude a minority of Si–Ga bonds, but we found strong, quantitative evidence for almost 1 ML Si-P bonds at the GaP/Si(100) interface.

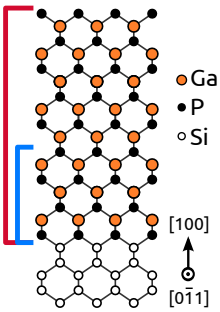

	5 PP		10 PP	
	E_B[eV]	C[ML]	E_B[eV]	C[ML]
P_1	129.55	3.30	129.54	8.1
P_2	**130.27**	**0.99**	**130.11**	**1.4**
Si_1	100.22	-	100.16	-
Si_2	**100.99**	**0.87**	**100.89**	**1.36**
	ΔE_B[eV]	R	ΔE_B[eV]	R
P_1:Si_2	28.56	4.50	28.65	9.97
P_2:Si_2	**29.28**	**1.18**	**29.22**	**1.09**

Figure 5: (left) Ball-and-stick model indicating quantification for 5 (blue bracket) and 10 PP (red bracket). (right) Binding energies and coverages C (quantified via a cross-sections and electron attenuation lengths) and ratios R (estimated via atomic sensitivity factors) for quantification.

The difference in P coverage of about 5 ML between 5 and 10 PP fits to adding half a lattice constant of GaP per PP (note that surfaces were TBP stabilized, so that the uppermost P layer is not to be counted as a pulse here) as indicated in the sketch in Fig. 5. Consequently, the nucleation is fully established after 3 PP. This is in line with the establishment of $\frac{\Delta r}{r}\big|_{\text{nucleation}}$ during the very first pulses as discussed above. The GaP coverage estimated via XPS for 5 PP agrees with the thickness of the nucleation layer of (0.6 ± 0.3) nm estimated from a linear fit of the growth rate from the GaP/Si(100) sample grown for IDA/SDA calculation.

According to Ref.,[41] we can estimate the valence band offset (VBO) from the measured Si/P $2p_{3/2}$ core level positions and the valence band maxima of the 10 PP sample, a Si(100) and a thicker GaP/Si(100) reference to VBO = (600 ± 150) meV. This value is lower than reported in literature.[42,43] The VBO will depend on the actual electronic interface structure so that comparison to theoretical modeling will enable further insight on the atomic interface structure.

In conclusion, we monitored the chemical arrangement of the buried GaP/Si(100) interface during nucleation of GaP on almost single-domain Si(100) time-resolved with *in situ* RAS. A characteristic, nucleation related dielectric anisotropy establishes already during the very first pulses at low temperature (420 °C). This optical anisotropy is consistent with the interface dielectric anisotropy calculated from RA spectra of thicker GaP/Si(100) heterostructures and is attributed to the heterointerface. We evidenced the existence of Si–P bonds with *in system* XPS which quantitatively correspond to about 1 ML. These findings agree with a kinetically limited formation of abrupt Si–P heterointerfaces suggested recently. Further, the *in situ* approach presented here enables detailed studies of the influence of variations of the chemical nucleation conditions on heterointerface formation.

Experimental methods

All samples were prepared in a horizontal AIX-200 MOCVD reactor equipped with a RA spectrometer (LayTec EpiRAS-200) for *in situ* control. A baseline accounting for setup intrinsic contributions was subtracted and the RAS amplitude is given with respect to a Si(110) reference. Silane (SiH_4), triethylgallium (TEGa) and tertbutylphosphine (TBP) were used as precursors and Pd-purified H_2 as process gas. GaP was nucleated pulsed at 420 °C on Si(100) 2° → [011] with A-type terraces.[3] For calculation of the IDA, a 5 PP nucleation sequence was followed by GaP growth at 595 °C (see Ref.[10] for parameters), which was interrupted by $(2 \times 2)/c(4 \times 2)$ surface preparation[29] and RAS measurements at

50 °C after 21 nm, 27 nm, 36 nm, and 48 nm total epilayer thickness. Temperatures given here were measured with a thermocouple placed inside the susceptor. After contamination-free transfer to UHV,[34] samples were analyzed with LEED (Specs ErLEED 100-A) and XPS (Specs Focus 500 and Phoibos 100 / 1D-DLD-43-100).

Dielectric anisotropies were measured with reflection anisotropy spectroscopy (RAS) which probes the difference

$$\frac{\Delta r}{r} = 2\,\frac{r_{[0\bar{1}1]} - r_{[011]}}{r_{[0\bar{1}1]} + r_{[011]}} \tag{2}$$

in complex reflection r along two mutually perpendicular axes.[12–14] For higher time resolution of the *in situ* measurement, a certain wavelength can be fixed (transient RA).

Based on Ref.s,[16,31,44] we derived a dielectric model to extract the surface dielectric anisotropies (SDA) and the buried interface dielectric anisotropy (IDA)—which are convoluted with interference and absorption in the RA spectra—from RAS data of two epilayers with different thicknesses.[15] This deconvolution approach requires (i) the real part of GaP/Si(100) RA spectra of two differently thick GaP epilayers, (ii) the corresponding imaginary RAS signals, (iii) the thicknesses of the epilayers and (iv) the dielectric functions of Si and GaP as input. Here, we measure the real parts of RAS during interrupted growth of one single sample and calculate their imaginary counterparts self-consistently via the Kramers-Kronig relation.[14] The GaP epilayer thickness results from a fit of the measured relative reflectance $R_{\mathrm{GaP/Si}} \,/\, R_{\mathrm{Si}}$, cf. Ref.,[45] for each growth step. Dielectric functions are taken from literature.[46,47] Anti-phase disorder was considered negligible due to the quasi single-domain character of the samples. Fig. 3 shows imaginary parts of SDA and IDA since they in first order relate to the real parts of the corresponding RAS signals.[44]

We fitted the XPS PE lines applying the open-source software *fityk*.[48] Voigt profiles were used as model functions and the background was approximated by a linear function. For each set of fit functions (such as the four components of a Si 2p fit), the full width at half-maximum was set identical for all peak components. The intensity ratio of each 2p doublet pair was fixed to 2:1.

Acknowledgments

The authors gratefully acknowledge valuable discussions with Sibylle Gemming, Benjamin Borkenhagen, Gerhard Lilienkamp, and Winfried Daum, as well as experimental support by Agnieszka Paszuk, Matthias Biester, Christian Höhn, and Antonio Müller. This work was financially supported by the DFG (proj. no. HA3096). MM. May and A. Nägelein appreciate PhD scholarships of the Studienstiftung des deutschen Volkes e.V. and Carl Zeiss Stiftung, respectively. O. Romanyuk acknowledges support by ASCR (proj. no. M100101201).

References

(1) Kroemer, H. Polar-on-Nonpolar Epitaxy. *J. Cryst. Growth* **1987**, *81*, 193–204.

(2) Kroemer, H. Nobel Lecture: Quasielectric Fields and Band Offsets: Teaching Electrons New Tricks. *Rev. Mod. Phys.* **2001**, *73*, 783–793.

(3) Brückner, S.; Döscher, H.; Kleinschmidt, P.; Supplie, O.; Dobrich, A.; Hannappel, T. Anomalous Double-Layer Step Formation on Si(100) in Hydrogen Process Ambient. *Phys. Rev. B* **2012**, *86*, 195310.1–195310.5.

(4) Brückner, S.; Kleinschmidt, P.; Supplie, O.; Döscher, H.; Hannappel, T. Domain-Sensitive In Situ Observation of Layer-by-Layer Removal at Si(100) in H_2 Ambient. *New J. Phys.* **2013**, *15*, 113049.1–113049.10.

(5) Dietz, N.; Rossow, U.; Aspnes, D.; Bachmann, K. J. Real-Time Optical Monitoring of Epitaxial Growth: Pulsed Chemical Beam Epitaxy of GaP and InP Homoepitaxy and Heteroepitaxy on Si. *J. Electron. Mater.* **1995**, *24*, 1571–1576.

(6) Wright, S. L.; Inada, M.; Kroemer, H. Polar-on-Nonpolar Epitaxy: Sublattice Ordering in the Nucleation and Growth of GaP on Si(211) Surfaces. *J. Vac. Sci. Technol.* **1982**, *21*, 534–539.

(7) Volz, K.; Beyer, A.; Witte, W.; Ohlmann, J.; Németh, I.; Kunert, B.; Stolz, W. GaP-Nucleation on Exact Si(001) Substrates for III/V Device Integration. *J. Cryst. Growth* **2011**, *315*, 37–47.

(8) Németh, I.; Kunert, B.; Stolz, W.; Volz, K. Heteroepitaxy of GaP on Si: Correlation of Morphology, Anti-Phase-Domain Structure and MOVPE Growth Conditions. *J. Cryst. Growth* **2008**, *310*, 1595–1601.

(9) Beyer, A.; Ohlmann, J.; Liebich, S.; Heim, H.; Witte, G.; Stolz, W.; Volz, K. GaP Heteroepitaxy on Si(001): Correlation of Si-Surface Structure, GaP Growth Conditions, and Si-III/V Interface Structure. *J. Appl. Phys.* **2012**, *111*, 083534.1–083534.6.

(10) Supplie, O.; Brückner, S.; Romanyuk, O.; Döscher, H.; May, M. M.; Stange, H.; Höhn, C.; Kleinschmidt, P.; Grosse, F.; Hannappel, T. Atomic Scale Analysis of the GaP/Si(100) Heterointerface by *In Situ* Reflection Anisotropy Spectroscopy and *Ab Initio* Density Functional Theory. *Phys. Rev. B* **2014**, *90*, 235301.1–235301.7.

(11) Steinbach, G.; Schreiber, M.; Gemming, S. DFT Investigation of the Heterostructure GaP(001) on Si(001). *Nanosci. Nanotechnol. Lett.* **2013**, *5*, 73–77.

(12) Aspnes, D. E.; Studna, A. A. Anisotropies in the Above-Band-Gap Optical Spectra of Cubic Semiconductors. *Phys. Rev. Lett.* **1985**, *54*, 1956–1959.

(13) Weightman, P.; Martin, D. S.; Cole, R. J.; Farrell, T. Reflection Anisotropy Spectroscopy. *Rep. Progr. Phys.* **2005**, *68*, 1251–1341.

(14) Zettler, J.-T. Characterization of Eepitaxial Semiconductor Growth by Reflectance Anisotropy Spectroscopy and Ellipsometry. *Prog. Cryst. Growth Ch.* **1997**, *35*, 27–98.

(15) Supplie, O.; Hannappel, T.; Pristovsek, M.; Döscher, H. In Situ Access to the Dielectric Anisotropy of Buried III-V/Si(100) Heterointerfaces. *Phys. Rev. B* **2012**, *86*, 035308.1–035308.5.

(16) Hunderi, O.; Zettler, J.-T.; Haberland, K. On the AlAs/GaAs(001) Interface Dielectric Anisotropy. *Thin Solid Films* **2005**, *472*, 261–269.

(17) Balderas-Navarro, R.; Hingerl, K.; Stifter, D.; Bonanni, A.; Sitter, H. Reflectance Difference Spectroscopy during CdTe/ZnTe Interface Formation. *Appl. Surf. Sci.* **2002**, *190*, 307–310.

(18) Sole, R. D.; Onida, G. Surface Versus Crystal-Termination Effects in the Optical Properties of Surfaces. *Phys. Rev. B* **1999**, *60*, 5523–5528.

(19) Chadi, D. J. Stabilities of Single-Layer and Bilayer Steps on Si(001) Surfaces. *Phys. Rev. Lett.* **1987**, *59*, 1691–1694.

(20) Shioda, R.; van der Weide, J. Observation of Hydrogen Adsorption on Si(001) by Reflectance Difference Spectroscopy. *Appl. Surf. Sci.* **1998**, *130-132*, 266–270.

(21) Palummo, M.; Witkowski, N.; Pluchery, O.; Del Sole, R.; Borensztein, Y. Reflectance-Anisotropy Spectroscopy and Surface Differential Reflectance Spectra at the Si(100) Surface: Combined Experimental and Theoretical Study. *Phys. Rev. B* **2009**, *79*, 035327.1–035327.8.

(22) Dietz, N.; Rossow, U.; Aspnes, D.; Bachmann, K. Real-Time Optical Monitoring of Epitaxial Growth: Pulsed Chemical Beam Epitaxy of GaP and InP Homoepitaxy and Heteroepitaxy on Si. *J. Cryst. Growth* **1996**, *164*, 34–39.

(23) Dietz, N.; Rossow, U.; Aspnes, D.; Bachmann, K. Real-Time Optical Monitoring of Heteroepitaxial Growth Processes on Si under Pulsed Chemical Beam Epitaxy Conditions. *Appl. Surf. Sci.* **1996**, *102*, 47–51.

(24) Zollner, S.; Garriga, M.; Kircher, J.; Humlícek, J.; Cardona, M.; Neuhold, G. Temperature Dependence of the Dielectric Function and the Interband Critical-Point Parameters of GaP. *Thin Solid Films* **1993**, *233*, 185–188.

(25) Lautenschlager, P.; Garriga, M.; Vina, L.; Cardona, M. Temperature Dependence of the Dielectric Function and Interband Critical Points in Silicon. *Phys. Rev. B* **1987**, *36*, 4821–4830.

(26) Sippel, P.; Supplie, O.; May, M. M.; Eichberger, R.; Hannappel, T. Electronic Structures of GaP(100) Surface Reconstructions Probed with Two-Photon Photoemission Spectroscopy. *Phys. Rev. B* **2014**, *89*, 165312.1–165312.8.

(27) Hahn, P. H.; Schmidt, W. G.; Bechstedt, F.; Pulci, O.; Sole, R. D. P-rich GaP(001)(2×1)/(2×2) Surface: A Hydrogen-Adsorbate Structure Determined from First-Principles Calculations. *Phys. Rev. B* **2003**, *68*, 033311.1–033311.4.

(28) Döscher, H.; Hannappel, T.; Kunert, B.; Beyer, A.; Volz, K.; Stolz, W. In situ Verification of Single-Domain III-V on Si(100) Growth via Metal-Organic Vapor Phase Epitaxy. *Appl. Phys. Lett.* **2008**, *93*, 172110–172113.

(29) Döscher, H.; Hannappel, T. In Situ Reflection Anisotropy Spectroscopy Analysis of Heteroepitaxial GaP Films Grown on Si(100). *J. Appl. Phys.* **2010**, *107*, 123523.1–123523.12.

(30) Töben, L.; Hannappel, T.; Möller, K.; Crawack, H.; Pettenkofer, C.; Willig, F. RDS, LEED and STM of the P-rich and Ga-Rich Ssurfaces of GaP(100). *Surf. Sci.* **2001**, *494*, L755–L760.

(31) Yasuda, T. Interface, Surface and Bulk Anisotropies of Heterostructures. *Thin Solid Films* **1998**, *313–314*, 544–551.

(32) Schmidt, W.; Esser, N.; Frisch, A.; Vogt, P.; Bernholc, J.; Bechstedt, F.; Zorn, M.; Hannappel, T.; Visbeck, S.; Willig, F. et al. Understanding Reflectance Anisotropy: Surface-State Signatures and Bulk-Related Features in the Optical Spectrum of InP(001)(2×4). *Phys. Rev. B* **2000**, *61*, 16335–16338.

(33) Hingerl, K.; Balderas-Navarro, R. E.; Bonanni, A.; Tichopadek, P.; Schmidt, W. G. On the Origin of Resonance Features in Reflectance Difference Data of Silicon. *Appl. Surf. Sci.* **2001**, *175–176*, 769–776.

(34) Hannappel, T.; Visbeck, S.; Töben, L.; Willig, F. Apparatus for Investigating Metalorganic Chemical Vapor Deposition-Grown Semiconductors with Ultrahigh-Vacuum Based Techniques. *Rev. Sci. Instrum.* **2004**, *75*, 1297–1304.

(35) May, M.; Lewerenz, H.-J.; Hannappel, T. Optical In Situ Study of InP(100) Surface Chemistry: Dissociative Adsorption of Water and Oxygen. *J. Phys. Chem. C* **2014**, *118*, 19032–19041.

(36) Yeh, J.; Lindau, I. Atomic Subshell Photoionization Cross Sections and Asymmetry Parameters: $1 < Z < 103$. *Atom Data Nucl. Data* **1985**, *32*, 1–155.

(37) Powell, C.; Jablonski, A. *NIST Electron Effective-Attenuation- Length Database* **2011**, *Version 1.3*.

(38) Bringans, R. D.; Olmstead, M. A.; Uhrberg, R. I. G.; Bachrach, R. Z. Summary Abstract: Core Level Spectroscopy of the GaAs-on-Si Interface. *J. Vac. Sci. Technol. A* **1987**, *5*, 2141–2142.

(39) Döscher, H.; Brückner, S.; Dobrich, A.; Höhn, C.; Kleinschmidt, P.; Hannappel, T. Surface Preparation of Si(100) by Thermal Oxide Removal in a Chemical Vapor Environment. *J. Cryst. Growth* **2011**, *315*, 10–15.

(40) Delplancke, M. P.; Powers, J. M.; Vandentop, G. J.; Salmeron, M.; Somorjai, G. A. Preparation and Characterization of Amorphous SiC:H Thin Films. *J. Vac. Sci. Technol. A* **1991**, *9*, 450–455.

(41) Waldrop, J. R.; Grant, R. W.; Kowalczyk, S. P.; Kraut, E. A. Measurement of Semi-

conductor Heterojunction Band Discontinuities by X-Ray Photoemission Spectroscopy. *J. Vac. Sci. Technol. A* **1985**, *3*, 835–841.

(42) Perfetti, P.; Patella, F.; Sette, F.; Quaresima, C.; Capasso, C.; Savoia, A.; Margaritondo, G. Experimental Study of the GaP-Si Interface. *Phys. Rev. B* **1984**, *30*, 4533–4539.

(43) Sakata, I.; Kawanami, H. Band Discontinuities in Gallium Phosphide/Crystalline Silicon Heterojunctions Studied by Internal Photoemission. *Appl. Phys. Express* **2008**, *1*, 091201.1–091201.3.

(44) McIntyre, J. D. E.; Aspnes, D. E. Differential Reflection Spectroscopy of Very Thin Surface Films. *Surf. Sci.* **1971**, *24*, 417–434.

(45) Haberland, K.; Kurpas, P.; Pristovsek, M.; Zettler, J.-T.; Weyers, M.; Richter, W. Spectroscopic Process Sensors in MOVPE Device Production. *Appl. Phys. A* **1999**, *68*, 309–313.

(46) Jellison Jr., G. Optical Functions of GaAs, GaP, and Ge Determined by Two-Channel Polarization Modulation Ellipsometry. *Opt. Mater.* **1992**, *1*, 151–160.

(47) Jellison Jr., G. Optical Functions of Silicon Determined by Two-Channel Polarization Modulation Ellipsometry. *Opt. Mater.* **1992**, *1*, 41–47.

(48) Wojdyr, M. *Fityk*: A General-Purpose Peak Fitting Program. *J. Appl. Cryst.* **2010**, *43*, 1126–1128.